Aerostatic Stiffness and Damping Analysis for High-Speed Air Bearings in Ultra-Precision Machine Tools

Author(s):
Stoop, Fabian; Mayr, Josef; Wegener, Konrad

Publication date:
2022

Permanent link:
https://doi.org/10.3929/ethz-b-000552303

euspen's 22nd International Conference & Exhibition, Geneva, CH, May/June 2022
www.euspen.eu

Aerostatic Stiffness and Damping Analysis for High-Speed Air Bearings in Ultra-Precision Machine Tools

Fabian Stoop[1], Josef Mayr[2], Konrad Wegener[1]

[1]*Institute of Machine Tools and Manufacturing (IWF), ETH Zürich, Zürich, Switzerland*
[2]*inspire AG, Zürich, Switzerland*

stoop@iwf.mavt.ethz.ch

Abstract

The microsystems technology drives manufacturing industries with the need for smaller structures for ultra-precision requirements. Precision combined with the allowed dynamics of the moving components are basic principles. Aerostatic bearings provide smooth and contactless movements, which are key resources for ultra-precision machine tools. Providing sufficient high stiffness properties for manufacturing applications, the air gap height of gas bearings has a size of just a few micrometres and shows a clear sensitivity to temperature and, in the case of journal bearings, also to speed. An algorithm developed computes the stiffness and damping properties and performs a full sensitivity analysis investigating all physical parameters of a plain journal bearing. The advanced approach combines a 2D-Thin-Film Finite Difference Method (FDM) with the Infinitesimal Perturbation Method (IFP) to achieve an eccentricity and attitude angle-dependent pressure distribution. This study describes a fully parametrized approach to serve as a base for the sensitivity analysis during the design phase and for the model of the control system. The outlined concept is evaluated on a high-speed journal bearing with the dimensionless DN factor of $3 \cdot 10^6$. The orifice design in combination with industry-standard inlet pressure ranges is the main design restriction. The described correlation matrices are evaluated with the Latin Hypercube Sampling Method and ensures together with the 2D Reynolds equation-based FDM algorithm a short calculation period. The proposed system is validated and further discussed through a rotor dynamic study on a high-speed aerostatic machine tool spindle.

Air bearing, ultra-precision machine tools, dynamic stiffness

1. Introduction

Air bearings are a key element in ultra-precision machining. Powell [1] described different bearing characteristics like aerostatic and aerodynamic bearings, orifice design and the corresponding analytical approximation. Whereas classic aerostatic bearings have to achieve increasingly stiffnesses with simultaneously smaller air consumption, only the air gap clearance can be reduced. The static effects, which are independent of speed, are superimposed by the dynamic behaviour. An essential feature is the increased load capacity with increasing speed. In addition to the characteristic deflection of the shaft, there is also a characteristic attitude angle. The description of this hybrid journal bearing behaviour is becoming increasingly important for high-speed journal bearing with maximum rotational speed times the nominal diameter as the dimensionless DN factor of $3 \cdot 10^6$.

Li et al. [2] investigated the analysis of roller bearing configuration effects on high-speed spindles using an integrated dynamic thermo-mechanical spindle model. The resulting behaviour of the stiffness and damping parameter illustrates the significance of such analysis in spindle design. For air bearing spindle this is also possible with the consideration of the air gap clearance variation depending on the temperature.

The procedure of solving a dynamic characterised air film is described by Yang et al. [3]. The focus is on the influence of the orifices, determining with the Perturbation Method to analyze the stability of the rotor behaviour. The basis for this investigation is the Reynolds equations. Kim et al. [4] formulated the generalised version of the Reynolds equation for an air bearing with curved bearing surfaces. This formulation aims to facilitate the dynamic calculation of air bearings of different shapes in operation.

The dependencies and operating conditions in a plain journal bearing alone are so diverse that an efficient calculation method is needed. Cui et al. [5] described the procedure for analysing the angular stiffness of a combined axial thrust and radial journal bearing. The Finite Element Method (FEM) is chosen for the calculation because it is less time-consuming and more efficient compared to Computational Fluid Dynamics (CFD).

Dupont [6] further elaborated the dynamic stability and robust rotor dynamics which lead to low errors in motion and vibrations. The combination of a computational efficient parametrized 2D-FDM-IFP simulation and a fully performed sensitivity analysis is shown for the first time in this work.

2. Method

The airgap hight is much smaller compared to the length and diameter of a hybrid plain journal bearing. Therefore the general Reynolds equation is applied according to Rowe [7]:

$$\rho\left(\frac{\partial u}{\partial t}+u\frac{\partial u}{\partial x}+v\frac{\partial u}{\partial y}+w\frac{\partial u}{\partial z}\right) = \rho g_x-\frac{\partial p}{\partial x}+\mu\left(\frac{\partial^2 u}{\partial x^2}+\frac{\partial^2 u}{\partial y^2}+\frac{\partial^2 u}{\partial z^2}\right) \quad (1)$$

$$\rho\left(\frac{\partial v}{\partial t}+u\frac{\partial v}{\partial x}+v\frac{\partial v}{\partial y}+w\frac{\partial v}{\partial z}\right) = \rho g_y-\frac{\partial p}{\partial y}+\mu\left(\frac{\partial^2 v}{\partial x^2}+\frac{\partial^2 v}{\partial y^2}+\frac{\partial^2 v}{\partial z^2}\right) \quad (2)$$

$$\rho\left(\frac{\partial w}{\partial t}+u\frac{\partial w}{\partial x}+v\frac{\partial w}{\partial y}+w\frac{\partial w}{\partial z}\right) = \rho g_z-\frac{\partial p}{\partial z}+\mu\left(\frac{\partial^2 w}{\partial x^2}+\frac{\partial^2 w}{\partial y^2}+\frac{\partial^2 w}{\partial z^2}\right) \quad (3)$$

The following assumptions are considered:

- The fluid is incompressible
- Constant fluid viscosity
- The body forces are neglected:

$$g_x = 0, g_y = 0, g_z = 0$$

- Thin film geometryis applied: $\frac{\partial P}{\partial y} = 0$
- The forces of inertia are neglected:

$$\rho\left(\frac{\partial u}{\partial t} + u\frac{\partial u}{\partial x} + v\frac{\partial u}{\partial y} + w\frac{\partial u}{\partial z}\right) = 0 \quad (4)$$

$$\rho\left(\frac{\partial v}{\partial t} + u\frac{\partial v}{\partial x} + v\frac{\partial v}{\partial y} + w\frac{\partial v}{\partial z}\right) = 0 \quad (5)$$

$$\rho\left(\frac{\partial w}{\partial t} + u\frac{\partial w}{\partial x} + v\frac{\partial w}{\partial y} + w\frac{\partial w}{\partial z}\right) = 0 \quad (6)$$

This leads to the simplified and dimensionless Reynolds equation in the form of:

$$\frac{\partial}{\partial \emptyset}\left(H^3\frac{\partial P}{\partial \emptyset}\right) + \frac{\partial}{\partial Z}\left(H^3\frac{\partial P}{\partial Z}\right) = \frac{\partial H}{\partial \emptyset} + 2\left(\dot{X}sin\emptyset + \dot{Y}cos\emptyset\right) \quad (7)$$

The dimensionless pressure: $P = \frac{p}{6\mu\omega}\left(\frac{c}{R}\right)^2$ (8)

The dimensionless hight: $H = h/c$ with the air gap hight *h* and the nominal clearance *c*.

The angular coordinate: $\emptyset$

The height of the air gap is given as a variable depending on the position in the air bearing. No-slip is assumed at the transition and a mass flow specification is also given at the inlet of the orifice. The eccentric position of the shaft within the bearing clearance is influenced by the load it carries as illustrated in Figure 1. The eccentricity converges until the load is balanced by the pressure generated in the air film.

The angle between the load axis, the y-axis in Figure 1, and the line connecting the centre of the bearing to the centre of the rotor are called the attitude angle $\emptyset_\circ$. With the Newton-Raphson Method, the attitude angle is calculated by starting with an initial estimate until convergence is reached.

The Infinitesimal Perturbation Method uses the partial derivatives of the bearing forces as described by Qiu [8]. There is a zero-order solution around which linearisation takes place. The first-order derivatives of the quantities after the displacements are the pre-factors to the small disturbance deflections. The forces, stiffnesses and damping are calculated as follows:

$$\begin{pmatrix} k_{xx} = \frac{\partial F_x}{\partial x} \\ k_{xy} = \frac{\partial F_x}{\partial y} \\ k_{yx} = \frac{\partial F_y}{\partial x} \\ k_{yy} = \frac{\partial F_y}{\partial y} \\ c_{xx} = \frac{\partial F_x}{\partial \dot{x}} \\ c_{xy} = \frac{\partial F_x}{\partial \dot{y}} \\ c_{yx} = \frac{\partial F_y}{\partial \dot{x}} \\ c_{yy} = \frac{\partial F_y}{\partial \dot{y}} \end{pmatrix} = -C_f \int_{\emptyset_\circ}^{\emptyset_2} \int_0^{L/R} \begin{pmatrix} P_x sin\emptyset \\ P_y sin\emptyset \\ P_x cos\emptyset \\ P_y cos\emptyset \\ P_{\dot{x}} sin\emptyset \\ P_{\dot{y}} sin\emptyset \\ P_{\dot{x}} cos\emptyset \\ P_{\dot{y}} cos\emptyset \end{pmatrix} dZd\emptyset \quad (9)$$

For the perturbated pressure the following factors are needed:

$$C_f = \frac{C_8}{c} \text{ for } k_{xx}, k_{xy}, k_{yx}, k_{yy} \quad (10)$$

$$C_f = \frac{C_8}{cf} \text{ for } c_{xx}, c_{xy}, c_{yx}, c_{yy} \quad (11)$$

$$C_8 = 6\mu\omega R^2\left(\frac{R}{c}\right)^2 \quad (12)$$

Which lead to the perturbated pressures:

$$P_x = \frac{\partial P}{\partial X}, P_y = \frac{\partial P}{\partial Y}, P_{\dot{x}} = \frac{\partial P}{\partial \dot{X}}, P_{\dot{y}} = \frac{\partial P}{\partial \dot{Y}} \quad (13)$$

Whereas X, Y are the perturbated rotor centre displacements in x- and y-direction and $\dot{X}, \dot{Y}$ are the perturbated rotor speeds in x- and y-direction. The solution scheme is comparable as described by Yang et al. [3].

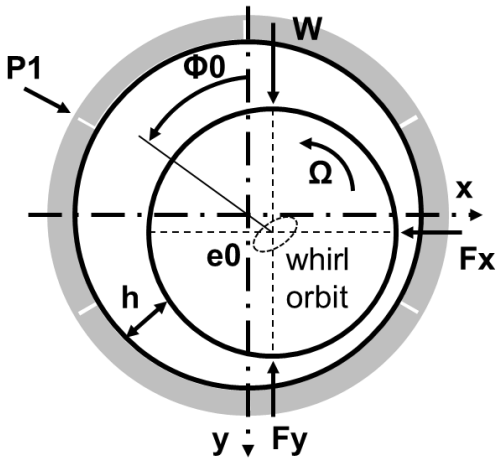

Figure 1: Schematic representation of the rotor movement

To analyse the influence of the design parameters on the stiffness and damping as well as on other dynamic parameters, it is necessary to consider a finite number of geometries. These geometries are chosen in such a way that on the one hand the interesting bandwidth is covered and on the other hand no linear dependencies arise between them. One approach for generating such design points is the Latin Hypercube Sampling Method (LHS). A manageable number of points are required while minimising the correlations between them as described by Zio [9].

3. Implementation

The described 2D representation of the pressure distribution in the air gap is now evaluated using FDM. The half-step FDM with the domain boundaries as described in Figure 2 is applied.

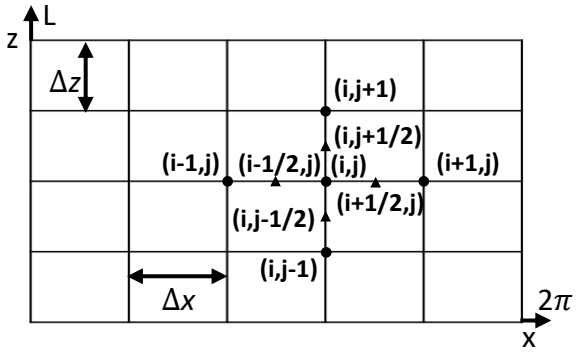

Figure 2: The applied half step Finite Difference Method (FDM) with the boundaries.

The manufacturing errors of a journal bearing due to the circumferential waviness is implemented according to Cui et al. [10]. The axial surface waviness has an influence on the static and dynamic characteristics of the journal bearing as described by Wang et al. [11]. The combination of axial and circumferential waviness error is elaborated from Wang et al. [12] and has a non-trivial dependency on both static and dynamic properties.

The main geometric bearing parameter and operational values for this analysis are listed in Table 1. The conditions for air have been idealised as standard conditions.

Table 1: Main journal bearing parameter

Parameter	Value	Unit	Description
R	18	mm	Nominal radius
c	40	µm	Nominal air gap
L	70	mm	Length of the bearing
p_s	5	bar	Supply pressure
p_a	1	bar	Ambient pressure
n_j	8	-	Number of orifices per column
n_r	2	-	Number of orifice columns
d_{or}	80	µm	Orifice diameter
ω_{max}	84'000	rpm	Max. rotational speed
μ	$1.79 \cdot 10^{-5}$	Ns/m²	Air viscosity
T	293	K	Air temperature
ρ	1.204	kg/m³	Air density
κ	1.4	-	Isentropic coefficient

4. Results

The results of the dynamic pressure distribution in the air gap of the journal bearing are shown in Figure 3. The pressure in the calculated 2D space is plotted where the boundary conditions reflect the continuity in both circumferential direction and the ambient pressure at the two axial outlets.

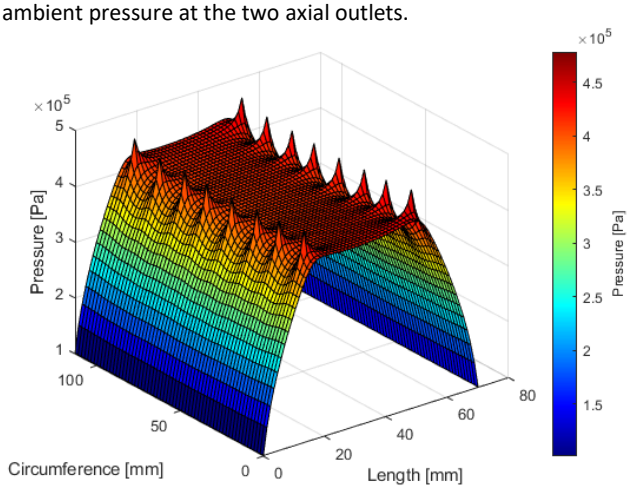

Figure 3: Pressure distribution in the air gap for the analyzed journal bearing.

Figure 4 also shows the pressure distribution for the given circumferential waviness. The increased pressures in the area of the smaller air gaps and the reduced pressures in the area of the larger air gaps can be seen.

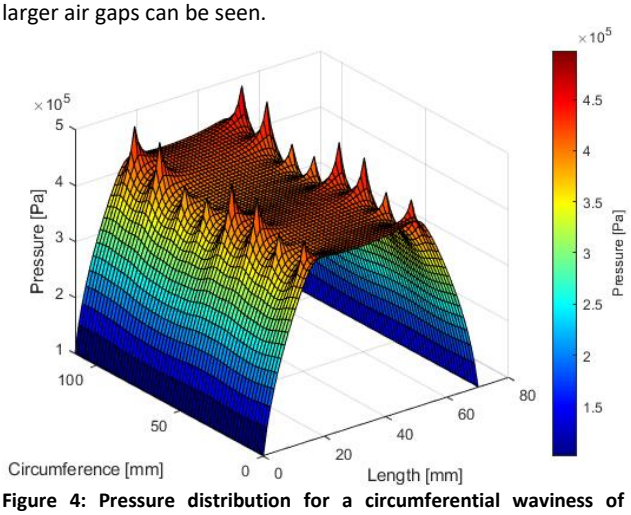

Figure 4: Pressure distribution for a circumferential waviness of amplitude 5 μm and waviness spatial number of 4.

Figure 5 also shows the pressure distribution at one eccentricity. A typical eccentricity of 0.1 is selected, which leads to the corresponding pressure distribution.

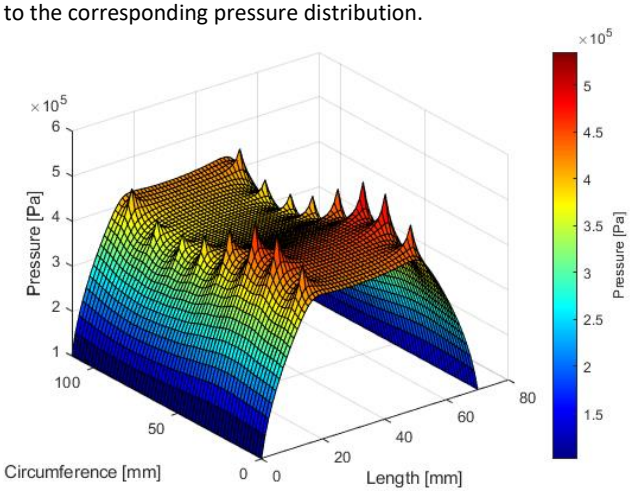

Figure 5: Pressure distribution with an eccentricity ratio of 0.1.

Figure 6 and Figure 7 show the characteristic dynamic values for the load capacity of the bearing and the stiffness. The strong correlation between load capacity and speed comes from aerodynamic effects with increasing speed. Furthermore, the stiffness in the YY-direction again shows a large dependence on the eccentricity, but only at high speeds, which is again due to the strong dynamic effects. The rotational speed goes up to the selected maximum speed and the deflection up to a relevant value of 0.2. The maximum rotational speed of 84'000 rpm times the nominal diameter of 36 mm represents the DN factor of $3 \cdot 10^6$.

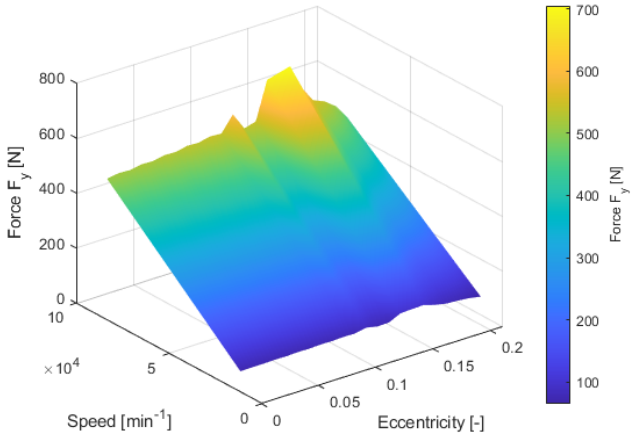

Figure 6: Dynamic force in y-direction based on the speed and eccentricity operating point

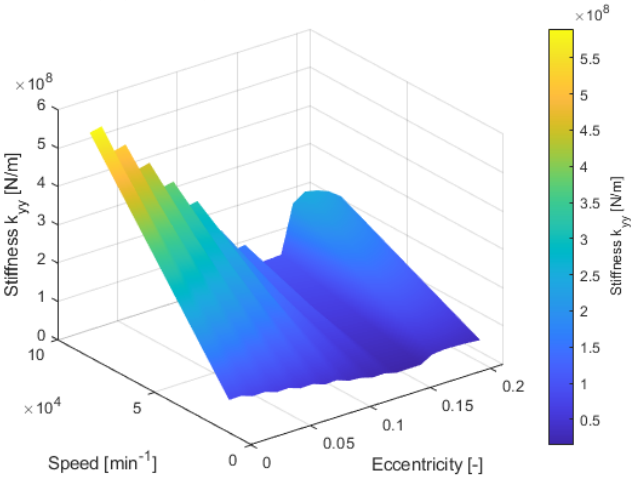

Figure 7: Stiffness based on the speed and eccentricity operating point

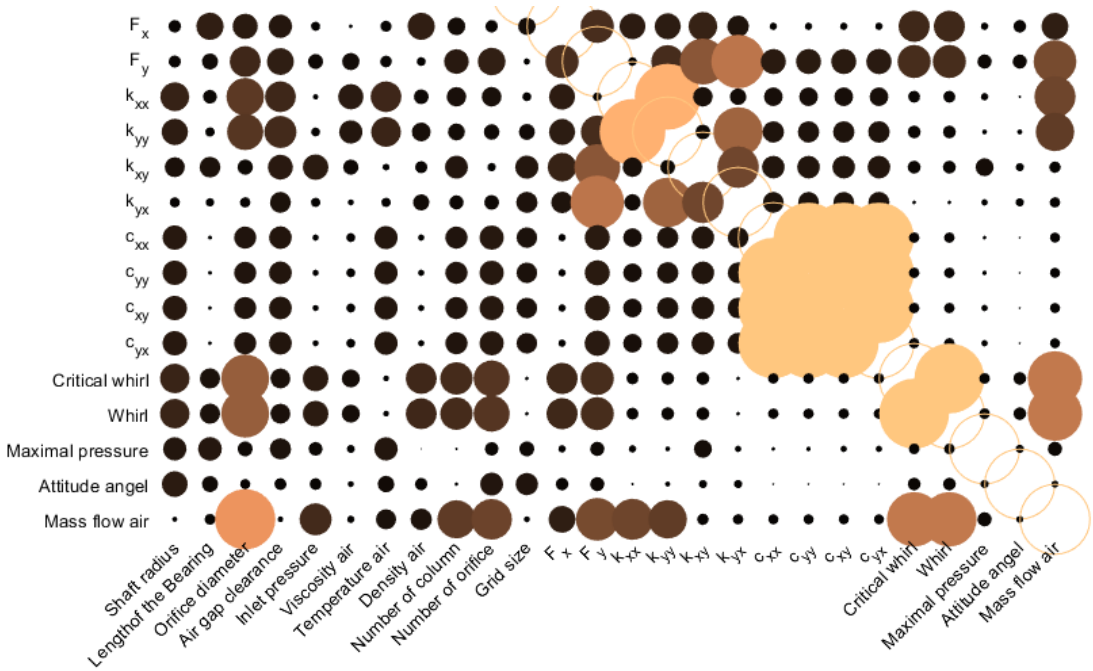

Figure 8: Matrix of sensitivities of the main journal bearing parameters on the dynamic properties. The brighter colours represent a positive correlation and the darker colours a negative correlation.

Figure 8 describes the sensitivity of the design parameters from the shaft radius to the number of nozzles with the resulting characteristic dynamic values.

For example, there is a strong correlation between the mass flow of the air and the nozzle diameter. This means that the larger the nozzle diameter, the greater the mass flow. This result is consistent with the physical behaviour of a flow restrictor. Furthermore, the nozzle diameter is also relevant for the whirl and the stiffness.

5. Discussion and Outlook

The parametric procedure for the aerostatic stiffness and damping analysis for high-speed air bearings is elaborated. The approach is based on the 2D Reynolds equation, which is solved with FDM and the Infinitesimal Perturbation Method.

The procedure allows an iterative formulation of the pressure distribution and air gap heights in the bearing gap, which are key-responsible for the dynamic behaviour. Furthermore, the procedure has high computational efficiency as it requires significantly less effort compared with the implementation in FEM or CFD. This enables efficient investigation considering a variety of different design points. The findings obtained with the help of this sensitivity analysis are important for obtaining fundamental design decisions when designing air bearing systems.

The developed approach shown can also be applied to other types of air bearing concepts such as thrust bearings and supports. The description of the air gap height function is different and usually easier than for bushings. Furthermore, the dynamic behaviour of the bearing and its sensitivity to other gases and liquids can be investigated efficiently by adjusting the parameters of the fluid. This efficient calculation of the aerodynamics part also enables a further integration into complex models for in-depth analysis such as rotor dynamics or thermodynamics.

References

[1] Powell JW (1970) Design of aerostatic bearings. Machinery Publishing

[2] Li H, Shin YC (2004) Analysis of bearing configuration effects on high speed spindles using an integrated dynamic thermo-mechanical spindle model. *Int J Mach Tools Manuf* **44:347–364** . https://doi.org/10.1016/j.ijmachtools.2003.10.011

[3] Yang DW, Chen CH, Kang Y, Hwang RM, Shyr SS (2009) Influence of orifices on stability of rotor-aerostatic bearing system. *Tribol Int* **42:1206–1219** . https://doi.org/10.1016/j.triboint.2009.04.002

[4] Kim H, Jang G, Ha H (2012) A generalized Reynolds equation and its perturbation equations for fluid dynamic bearings with curved surfaces. *Tribol Int* **50:6–15** . https://doi.org/10.1016/j.triboint.2011.12.019

[5] Cui H, Wang Y, Yang H, Zhou L, Li H, Wang W, Zhao C (2018) Numerical analysis and experimental research on the angular stiffness of aerostatic bearings. *Tribol Int* **120:166–178** . https://doi.org/10.1016/j.triboint.2017.12.040

[6] Dupont R (2015) Robust rotor dynamics for high-speed air bearing spindles. *Precis Eng* **40:7–13** . https://doi.org/10.1016/j.precisioneng.2014.12.008

[7] Brian Rowe W (2012) Hydrostatic, Aerostatic and Hybrid Bearing Design. Elsevier Inc.

[8] Qiu Z (1995) A Theoretical and Experimental Study on the Dynamic Characteristics of Journal Bearings. Doctoral Thesis, University of Wollongong

[9] Zio E (2013) The Monte Carlo Simulation Method for System Reliability and Risk Analysis. Springer London

[10] Cui H, Wang Y, Yue X, Huang M, Wang W, Jiang Z (2018) Numerical analysis and experimental investigation into the effects of manufacturing errors on the running accuracy of the aerostatic porous spindle. *Tribol Int* **118:20–36** . https://doi.org/10.1016/j.triboint.2017.09.020

[11] Wang X, Xu Q, Huang M, Zhang L, Peng Z (2017) Effects of journal rotation and surface waviness on the dynamic performance of aerostatic journal bearings. *Tribol Int* **112:1–9** . https://doi.org/10.1016/j.triboint.2017.03.027

[12] Wang X, Xu Q, Wang B, Zhang L, Yang H, Peng Z (2016) Effect of surface waviness on the static performance of aerostatic journal bearings. *Tribol Int* **103:394–405** . https://doi.org/10.1016/j.triboint.2016.07.026